Journal of Immunological Methods 368 (2011) 54–63

Contents lists available at ScienceDirect

Journal of Immunological Methods

journal homepage: www.elsevier.com/locate/jim

Research paper

Visualization and quantification of cytotoxicity mediated by antibodies using imaging flow cytometry

Gustavo Helguera [a,b,*], José A. Rodríguez [a,c], Rosendo Luria-Pérez [a,d], Shannon Henery [e], Paul Catterton [e], Carlos Bregni [b], Thaddeus C. George [e], Otoniel Martínez-Maza [f,g,h], Manuel L. Penichet [a,c,g,h]

[a] Division of Surgical Oncology, Department of Surgery, David Geffen School of Medicine, University of California, Los Angeles, CA, USA
[b] Department of Pharmaceutical Technology, School of Pharmacy and Biochemistry, University of Buenos Aires, Argentina
[c] Molecular Biology Institute, University of California, Los Angeles, CA, USA
[d] Unit of Investigative Research on Oncological Disease, Children's Hospital of Mexico "Federico Gómez", Mexico City, Mexico
[e] Amnis Corporation, Seattle, WA, USA
[f] Department of Obstetrics and Gynecology, David Geffen School of Medicine, University of California, Los Angeles, CA, USA
[g] Department of Microbiology, Immunology, and Molecular Genetics, David Geffen School of Medicine, University of California, Los Angeles, CA, USA
[h] Jonsson Comprehensive Cancer Center, University of California, Los Angeles, CA, USA

ARTICLE INFO

Article history:
Received 26 October 2009
Received in revised form 6 January 2011
Accepted 10 March 2011
Available online 21 March 2011

Keywords:
Antibody
ADCC
Immunotherapy
Cancer
Imaging flow cytometry

ABSTRACT

Conventional approaches for the detection of antibody dependent cell-mediated cytotoxicity (ADCC) activity rely on quantification of the release of traceable compounds from target cells or flow cytometry analysis of population-wide phenomena. We report a new method for the direct imaging and quantification of ADCC of cancer cells. The proposed method using imaging flow cytometry combines the statistical power of flow cytometry with the analytical advantages of cell imaging, providing a novel and more comprehensive perspective of effector/target cell interactions during ADCC events. With this method we can quantify and show in detail the morphological changes in target and effector cells, their apoptotic index, the physical interaction between effector and target cells, and a directional transfer of cytosolic contents from effector to target cells. As a model system we used the therapeutic anti-CD20 antibody rituximab to target CFSE labeled Ramos human Burkitt's lymphoma cells, to CMTPX-labeled human monocytic U-937 effector cells. We expect that similar studies using different effector and target cell populations may contribute to the pre-clinical evaluation of therapeutic antibodies and help to identify mechanisms that could be beneficial in the immunotherapy of cancer.

1. Introduction

In recent years the generation of therapeutic antibodies has experienced significant growth, a trend that is expected to continue, with many new developments in antibody engineering focused on the improvement of antibody effector functions (Wang and Weiner, 2008). In particular, the mechanism of antibody dependent cell-mediated cytotoxicity (ADCC) has been shown to play a major role in the therapeutic activity of rituximab (Rituxan™, Roche), trastuzumab (Herceptin™, Roche) and other monoclonal antibodies in development. Studies suggest that enhanced antibody

Abbreviations: ADCC, antibody-dependent cell-mediated cytotoxicity; ADCP, antibody-dependent cell mediated phagocytosis; E:T, effector to target ratio; CFSE, carboxy-fluorescein diacetate, succinimidyl ester; DRAQ5, 1,5-bis{[2-(di-methylamino) ethyl]amino}-4,8-dihydroxyanthracene-9,10-dione; LDH, lactate dehydrogenase; EDF, extended depth of field; FBS, fetal bovine serum; NHL, non-Hodgkin's lymphoma.

* Corresponding author at: Department of Pharmaceutical, Technology, School of Pharmacy and Biochemistry, University of Buenos Aires, 956, Junín Ave., 6th Floor; C1113AAD, Buenos Aires, Argentina. Tel./fax: +54 11 4964 8371.
E-mail address: ghelguera@ffyb.uba.ar (G. Helguera).

0022-1759/$ – see front matter © 2011 Elsevier B.V. All rights reserved.
doi:10.1016/j.jim.2011.03.003

mediated effector/target cell interactions and their cytotoxic effects on the target cells correlate with better overall response to treatment (Dalle et al., 2008). ADCC mediates the elimination of cancer cells through a mechanism that requires the presence of the antibody, target cells (expressing the antigen), and effector cells (bearing Fcγ-receptors) such as macrophages, NK cells, monocytes, or neutrophils. In the case of rituximab, it has been reported that leukemic target cells opsonized with antibody can be phagocytosed by macrophage effector cells (Glennie et al., 2007; Leidi et al., 2009). In vitro studies that aid in the prediction of clinical efficacy and in understanding the mode of action of therapeutic antibodies targeting cancer cells are of growing interest.

Current methods for ADCC determination rely on the evaluation of the loss of cell membrane integrity by quantification of the release of traceable compounds from target cells or by evaluation of the target cell viability by flow cytometry. The ^{51}Chromium (^{51}Cr) release assay relies on the quantification of the radioactive material liberated from ^{51}Cr-loaded target cells. It is a sensitive method and has been considered the gold standard for cell-mediated cytotoxicity (Brunner et al., 1968). However, its dependence on radioactivity, the variability in labeling efficacy, and substantial spontaneous leakage of the ^{51}Cr label in certain cell types has limited the usefulness of this method (Jakubek et al., 1983; Wisecarver et al., 1985). One non-radioactive alternative to the ^{51}Cr assay is the quantification of release of the fluorescent dye calcein-AM from target cells (Metelitsa et al., 2002). Another alternative is the colorimetric lactate dehydrogenase (LDH) assay which measures enzyme release after disruption of the cell membrane. It has the advantage that it is colorimetric and non-radioactive, but in ADCC assays this method does not differentiate target from effector cell-derived LDH release. Flow cytometry has also been used to measure cytotoxicity based on the uptake of DNA fluorescent probes after the disruption of the plasma membrane of target cells. This method has also been used for the simultaneous determination of ADCC and phagocytosis (ADCP) in three-color flow cytometry assays (Karagiannis et al., 2007). Although this method can effectively discriminate the viability of the subpopulations of effector cells, target cells, and interacting effector–target cells, it cannot distinguish effector–target conjugates from events in which the effector cell has phagocytosed the target. Fluorescence microscopy is used to discriminate these two cases, but this technique can miss rare events and has limited statistical power due to the limited number of events that can be analyzed.

To comprehensively evaluate ADCC activity and effector/target cell interactions in the presence of therapeutic antibodies we used the ImageStream imaging flow cytometry technology (Amnis Corp., Seattle, WA). This technology collects multiple high-resolution images (darkfield, brightfield, and various fluorescent) per cell in flow at high rates of image capture, enabling statistically robust microscopy applications. This technology has been used previously to measure simultaneously NK cytotoxicity and the phenotype of effector cells (Kim et al., 2007), to determine chemically induced apoptosis in cancer cell lines (George et al., 2004) and to study the membrane exchange between effector and target cells in the process of trogocytosis (Megjugorac et al., 2007; Beum et al., 2008). Here we used this technology to monitor simultaneously the viability of target cells, effector cells, and to analyze a subset of interacting effector/target cells, providing a novel and more comprehensive perspective of ADCC events mediated by a therapeutic antibody.

2. Materials and methods

2.1. Cell lines, fluorescent dyes, and antibody

The human monocytic cell line U-937 and the human Burkitt's B-cell lymphoma cell line Ramos were purchased from American Type Culture Collection (ATCC, Manassas, VA). Both cell lines were grown in RPMI 1640 medium (Life Technologies, Carlsbad, CA) supplemented with 100 U/ml penicillin, 10 μg/ml streptomycin, and 10% (v/v) heat inactivated fetal bovine serum (FBS) (Atlanta Biologicals, Atlanta, GA) at 37 °C in 5% CO_2. CellTracker™ Red (CMTPX, excitation 577 nm/emission of 602 nm) fluorescent dye (Molecular Probes, Life Technologies) was used to label the effector cells U-937 by incubating 30 min in the presence of RPMI 1640 with 10% FBS with 2 μM CMTPX at 37 °C in 5% CO_2. The cells were washed twice and further incubated for 30 min in RPMI 1640 with 10% FBS to remove the excess dye. Carboxyfluorescein succinimidyl ester (CFSE green, excitation 492 nm/emission of 517 nm) fluorescent dye (Molecular Probes, Life Technologies) was used to stain the target Ramos lymphoma cells. Briefly, cells were washed, resuspended 0.1% BSA in PBS with 0.2 μM CFSE and incubated 5 min at 37 °C. The reaction was quenched by adding 5 volumes of ice-cold 5% FBS in PBS and incubated for 5 min on ice. Cells were then washed twice with 5% FBS in PBS and resuspended in the growth media for the experiment. The mouse/human chimeric anti-CD20 IgG1 rituximab was purchased from Genentech (Genentech, San Francisco, CA).

2.2. Incubation of effector and target cells with the antibody

A total of 10^6 U-937 human monocyte effector cells labeled with the CMTPX red fluorescent dye were incubated with 2×10^5 Ramos human Burkitt's B-cell NHL target cells stained with the CFSE green fluorescent dye (5:1—E:T ratio) in the presence or absence of 5 μg/ml of rituximab for 1 h or 2 h at 37 °C in 5% CO_2. We used 5 μg/ml concentration of rituximab because it has been reported to be in the range to achieve ADCC activity (Manches et al., 2003). After the incubation, the cells were washed and fixed with 2% paraformaldehyde in PBS and the nuclei were stained with the DRAQ5 dye (1,5-bis{[2-(dimethylamino) ethyl]amino}-4, 8-dihydroxyanthracene-9,10-dione, Biostatus, Ltd., Leicestershire, UK) diluted 1/200 (12.5 μM, final concentration) for 30 min. We used DRAQ5 nuclear dye because it can stain nuclei of live or dead fixed cells.

2.3. Data acquisition with ImageStream

Samples were run in the ImageStream multispectral imaging flow cytometer (Amnis Corporation, Seattle, WA) and images were acquired for 10,000 events/sample. Cells were excited using a 488 nm laser with intensity ranging from 75 to 200 mW, depending on the staining. Brightfield, side scatter, fluorescent cell images were acquired at 40×

magnification. Only events with brightfield areas greater than 50 μm^2 (excludes debris) and non-saturating pixels were collected as previously described (Henery et al., 2008). Imagery of excluded events was observed to prevent the potential loss of events of interest. Single color controls were acquired to generate a compensation matrix that was applied to all experimental files prior to analysis.

2.4. Determination of apoptosis in effector and target cells

Apoptotic cells were identified by quantitative measurement of nuclear morphology, including nuclear texture, condensation, and fragmentation using the IDEAS® (Image Data Exploration and Analysis Software) package as previously described (Henery et al., 2008). For CFSE$^+$ (target) or CMTPX$^+$ (effector) cells, a nuclear mask was generated that contains only pixels with intensity values in the upper 40% of the intensity range of the DRAQ5 image. The area of this mask (Area T40% DRAQ5) in square microns is plotted as the abscissa in a bivariate plot against "Bright Detail Intensity R3", which measures the total intensity of small regions of localized staining (Beum et al., 2006). Apoptotic cells with condensed and fragmented nuclei have low Area T40% and high bright detail intensity values and thus can be gated on this plot (Henery et al., 2008). This analysis was used to quantify apoptotic CMTPX$^+$ and CFSE$^+$ events in the presence or absence of therapeutic antibody. The percentage of rituximab-induced apoptosis in target cells in the presence of effector cells was determined as the percentage of remaining viable cells with rituximab as compared to cells without the antibody incubated in the presence of the effector cells. The determination of percentage of apoptotic effector cells was calculated as the percentage of apoptotic CMTPX$^+$ events over the total number of events CMTPX$^+$ in the same condition.

2.5. Analysis of interactions between effector cells (CMTPX$^+$) and target cells (CFSE$^+$)

Images of double-positive events CMTPX$^+$/CFSE$^+$ in all experimental conditions were analyzed to visualize and quantify effector–target cell contact and phagocytosis using the IDEAS® package. To determine phagocytosis of target cells by effector cells, we measured the distance between the center of the CMPTX and CFSE images of double positive events using the Delta Centroid XY (DC) feature. Events in which effectors have phagocytosed target cells have significantly lower DC values compared to conjugate events. In cases where the DC is shorter than the radius of both images reaching a 3 μm threshold, it was considered to be in the phagocytosis/internalization event range. A histogram was generated for the DC values of the CMTPX$^+$/CFSE$^+$ events.

2.6. Statistical analysis

Significant differences in the data were determined by the student's *t*-test using Microsoft Excel 2004 (Microsoft Co., Redmond, WA, USA), with $p \leq 0.05$ considered to be significant.

3. Results

3.1. Controls and assay set up

To distinguish the events corresponding to the populations of effector, target and effector–target complexes we performed our analysis using bivariate plots. The analysis of the treatment with rituximab compared to buffer control was performed comparing the intensity of fluorescence in the green channel versus the intensity of the red channel. Fig. 1 shows a dot plot of cells incubated in the presence of rituximab where on the upper left corner U-937 CMTPX$^+$ cells are segregated in red with an inset of the percentage of the events in this quadrant. The arrow pointing down shows sample imagery of events in this quadrant in red fluorescence (CMTPX), brightfield, and DRAQ5 nuclear stain. On the bottom right corner of the plot are gated CFSE$^+$ events in green and a sample of events in this quadrant in green fluorescence (CFSE), brightfield, and DRAQ5 is shown below. On the upper right corner are gated double positive events and its percentage over the total event count. The arrow pointing up shows images of double positive events of effector and target cells in contact. In dark blue are shown CFSE$^+$ events above the threshold of CMTPX, but that are not "true" double positive events. The Ramos cells are shown in green, and U937 cells in red, DRAQ5 is the nuclear stain for both cell types, and is shown also in the overlay of the fluorescence and the overlay of brightfield, CFSE and CMTPX.

3.2. Determination of apoptosis in target and effector cells

Quantification of the apoptotic index within the populations of target and effector cells was performed by analysis of nuclear morphology parameters such as nuclear condensation, texture, and fragmentation using the IDEAS® package. Fig. 2A to F shows the steps that we followed to generate the series of masks to identify an apoptotic target cell in images of a dimeric effector/target event (Fig. 2A, B, and C). Once the CFSE$^+$ green target cell is identified and the mask applied, we identify the target cell nucleus stained with DRAQ5 (Fig. 2D and E). In the region containing the nucleus of interest, a threshold mask is then applied to the DRAQ5 nuclear image only under the CFSE$^+$ region to determine the apoptotic index in the target cell (Fig. 2F). Note the fragmentation and condensation of fluorescence signal in the nucleus area with high DRAQ5 intensity, considered evidence of apoptosis. In contrast, we show in Fig. 2G–H images of an effector/target event in which the target cell exhibits a homogeneous DRAQ5 staining (Fig. 2H). In this case there is no condensation or fragmentation of the nucleus and no granularity in the cytoplasm as would be expected inside a healthy, non-apoptotic cell. Fig. 3 shows the scatter plot with the morphologic metrics to determine the apoptotic index of CFSE$^+$ Ramos target cells incubated for 2 h with effector cells and rituximab. The gating of apoptotic and non apoptotic events of the CFSE$^+$ population were determined based on images of the DRAQ5 stained nucleus, where the area of the 40% threshold DRAQ5 nuclear mask within the Ramos cell was plotted as a parameter on the Y-axis versus bright detail intensity R3 on the X-axis. This is a "texture" feature in the IDEAS® software package that measures the amount of

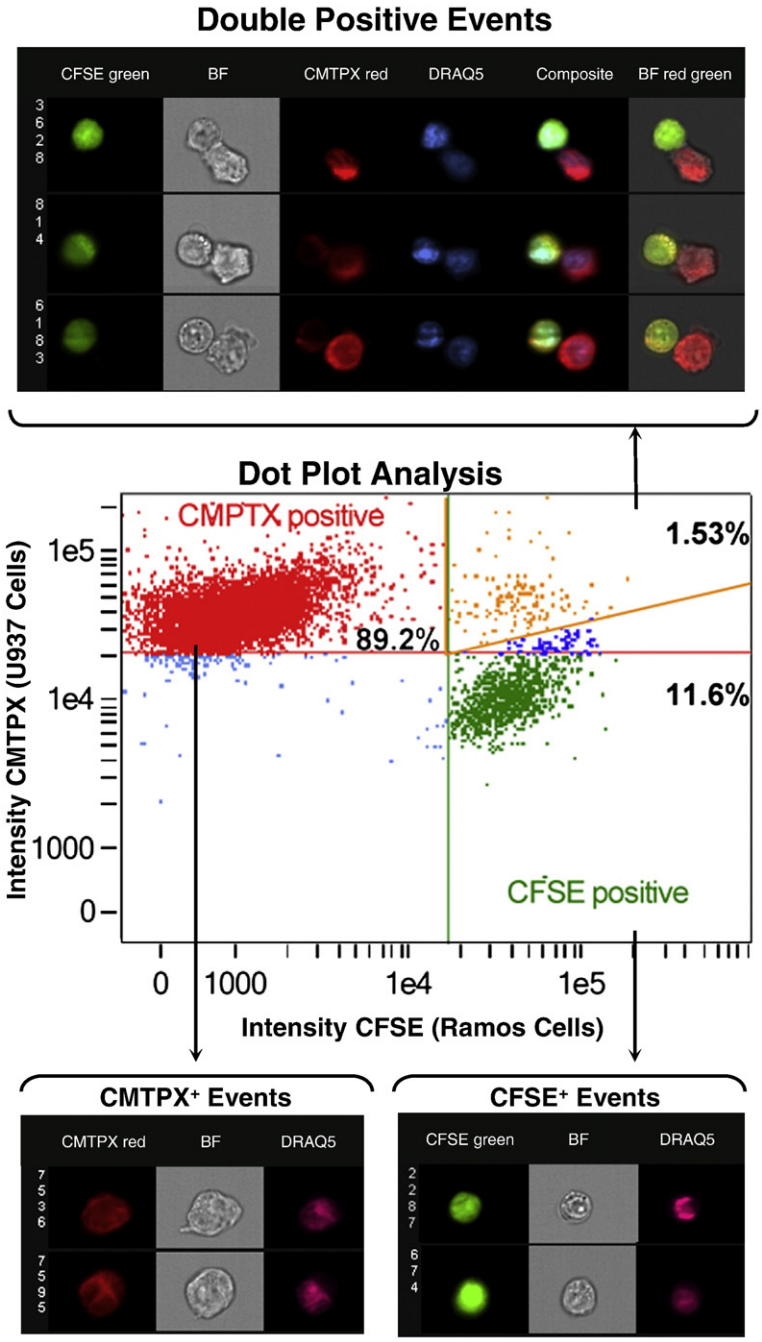

Fig. 1. Identification of effector and target cells by imaging flow cytometry. Standard dot plot analysis was used to determine red and green fluorescence intensity in U-937 human monocyte effector cells labeled red with the CMTPX fluorochrome co-incubated for 2 h with Ramos human Burkitt's B-cell NHL target cells labeled green with the CFSE fluorochrome (5:1—E:T ratio) in the presence of 5 μg/ml rituximab. After incubation, cells were fixed and nuclei stained with the DRAQ5 dye. Samples were run in the ImageStream and imagery acquired for 10,000 events. In the middle of the figure we show the dot plot of the treatment with the percentage of events $CMTPX^+$ in the upper left quadrant, $CFSE^+$ in the bottom right quadrant, and $CMTPX^+/CFSE^+$ in the top right quadrant. Above the dot plot we show representative imagery of double positive events from the upper right quadrant of the dot plot with CFSE fluorescence (CFSE green), brightfield (BF), CMTPX fluorescence (CMTPX red), DRAQ5 fluorescence (DRAQ5), CFSE, CMTPX, and DRAQ5 fluorescence (composite), and brightfield, CFSE and CMTPX fluorescence (BF red green). Below left we show representative imagery of single U-937 cells CMTPX positive from the upper left quadrant of the dot plot with CMTPX red, BF, and DRAQ5 pictures. And finally, below right we show representative imagery of single Ramos cells CFSE positive from the bottom right quadrant of the dot plot with CFSE green, BF, and DRAQ5 pictures.

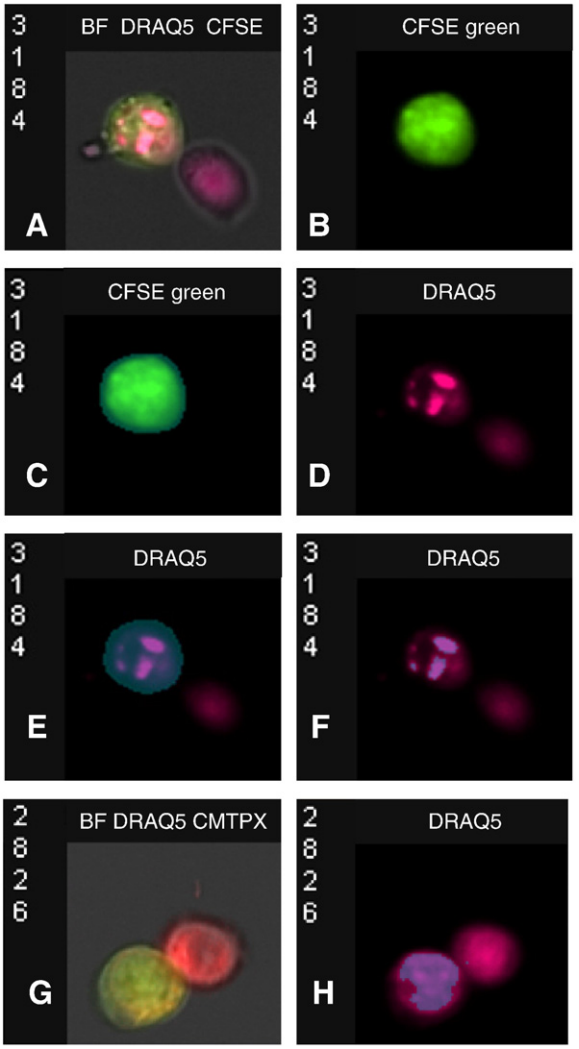

Fig. 2. Image analysis to determine apoptotic cells in double positive events. Panels A to F show the image analysis of nuclear morphology with the IDEAS® software used to determine the apoptotic status of a Ramos target cell in contact with a U-937 cell. Panel A shows a double positive event in which an apoptotic Ramos target cell is in contact with the U-937 effector cell in an overlay of the brightfield image together with CFSE and DRAQ5 fluorescence. Panel B shows the CFSE green fluorescence of the target cell, and panel C shows the mask created to identify the target cell. Panel D shows DRAQ5 fluorescent staining of the event and panel E the mask containing the fluorescent area of the condensed nucleus of the apoptotic cell. Panel F shows the threshold that identifies only the pixel values which fall in the brightest 40% of the range of pixel values found within the nucleus of the Ramos cell. Panels G and H show a double positive event in which the target cell is non-apoptotic. Panel G shows the DRAQ5 staining and the mask indicating the homogeneous nucleus of the healthy target cell, and panel H an overlay image of the event in brightfield, CFSE and CMTPX fluorescence channels.

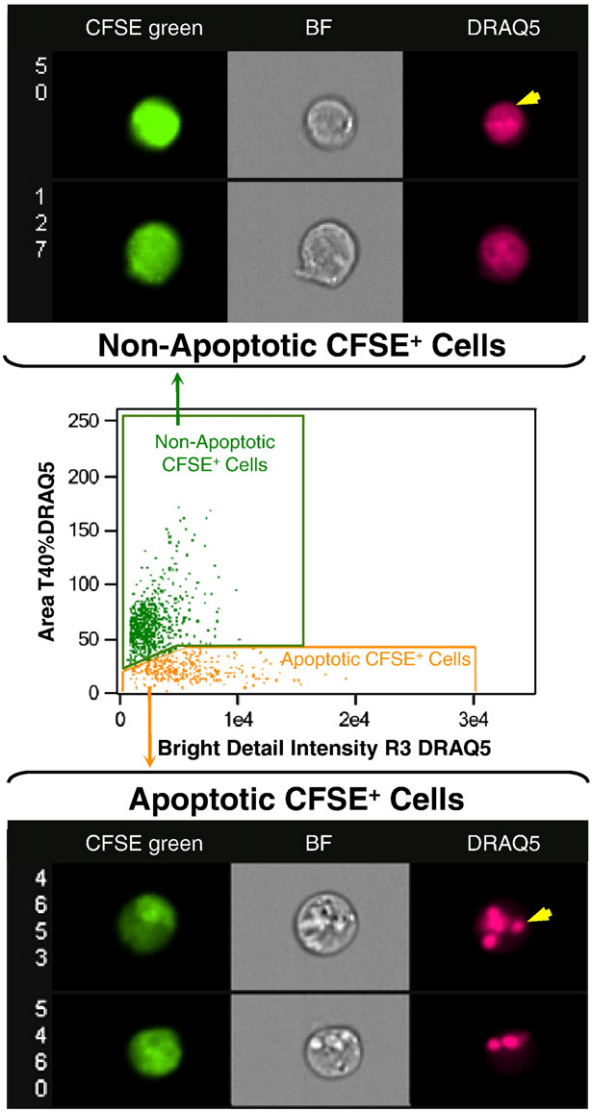

Fig. 3. Determination of apoptotic index by nuclear morphology. At the center is a bivariate plot analysis using the IDEAS® software showing Area threshold 40% DRAQ5 intensity versus bright detail intensity R3 DRAQ5 parameters of Ramos cells labeled with CFSE co-incubated for 2 h with U-937 effector cells in the presence of 5 μg/ml rituximab. The non-apoptotic Ramos $CFSE^+$ cells are gated in green. Sample CFSE, brightfield and DRAQ5 imagery are shown on top, with the yellow triangle pointing to the homogeneous nucleus stained with DRAQ5 typical of non-apoptotic cells. Apoptotic $CFSE^+$ cells are shown in orange, and representative CFSE, brightfield and DRAQ5 images are shown on the bottom, with the yellow triangle pointing to the nucleus fragmented and intensely stained with DRAQ5, typical of apoptotic cells. Note also in BF images the change in morphology, with intense granularity of the cytoplasm.

remaining bright signal with a radius of 3 pixels or less after subtraction of the detail eroded image, a parameter that is representative of level of granularity in the mask for the DRAQ5 image and correlates with the level of apoptosis of the cell (Henery et al., 2008). On top of the plot representative imagery of non-apoptotic $CFSE^+$ target cells is shown and below the plot apoptotic $CFSE^+$ target Ramos cells are shown. Similar procedures applied to single and dimeric $CMTPX^+$ events allow the identification of the apoptotic effector cells, and the discrimination between apoptotic effector and target cells in single and double positive events to estimate more accurately their apoptotic index.

3.3. Determination of total count and apoptotic index

The action of the effector cells in the presence of a therapeutic antibody can result in the total destruction and

Table 1
Three independent experiments showing total event count and percentage of CFSE$^+$ target Ramos cells after two hour incubation with rituximab in the presence of U-937 effector cells.

Experiment	Total counts (CFSE$^+$ count)		% CFSE$^+$ cells		Cell ratio rituximab/buffer
	Buffer	Rituximab	Buffer	Rituximab	
1	7052 (1468)	10,000 (901)	20.82	9.01	0.43
2	10,001 (1818)	10,000 (1625)	18.18	16.25	0.89
3	10,000 (1747)	10,000 (961)	17.47	9.61	0.55
Average			**18.82**	**11.62**	
Standard deviation			1.76	4.02	
t-test			0.047		

fragmentation of target cells to a level that they cannot be distinguished from debris. This activity can be quantified by the determination of the total count of remaining healthy target cells in the presence of effector cells and in the absence or the presence of the therapeutic antibody as an evidence of ADCC activity. For this purpose, a total of ten thousand events were acquired at 2 h in the presence or absence of rituximab at a 5:1 ratio of CMTPX$^+$ U-937 effector cells compared to CFSE$^+$ Ramos target cells. The comparison was made between antibody treated and buffer treated target cells to discard cell killing by effector cells not mediated by antibody and by spontaneous apoptosis of the target cells (Table 1). As expected, in the presence of rituximab a significant percentage of target cells are lost compared to buffer control (Table 1, Fig. 4A), which is interpreted as evidence of their destruction by ADCC. Since the quantified events of the target cell population include apoptotic cells (gray fraction in Fig. 4A), the proportion of healthy Ramos cells is lower compared with the total count of events and decreases as depicted in the white area in Fig. 4A for buffer treated versus rituximab treated cells. In the case of rituximab treated Ramos cells in the presence of U-937 effector cells, after 2 h incubation nearly one-fourth of the total CFSE$^+$ events detected were apoptotic cells. In contrast, we observed that the number of apoptotic effector cells was reduced by no more than 2% either in the presence of rituximab or in buffer control. These observations demonstrate that this method allows the simultaneous quantification of the apoptotic status of effector and target cell populations under different conditions, providing a more comprehensive evaluation of ADCC activity. Current methods ignore the status of the effector cells in this activity and may overlook some potential toxicity on effector cells that might jeopardize the therapeutic benefit of the antibody tested.

3.4. Cytoplasmic transfer from effector to target cells

Analysis of images of double positive events CMTPX$^+$/CFSE$^+$ also enables the observation of CMTPX$^+$ cytoplasmic signal present within CFSE$^+$ cells (Fig. 5A). In all cases, the overlap of the red signal was on the area of the target cells, which in some cases covered a large portion (>75% green area) of the green signal within the Ramos cells (Fig. 5A and B). In contrast, we did not observe cases of green cytoplasmic signal transferred into red effectors cells, suggesting that the transfer of cytoplasmic material occurred from effector to target cells, as would be expected in cases of ADCC activity. This observation is consistent with an ADCC activity in which the antibody facilitates this interaction between the effector and the target cells, an activity that also occurs spontaneously, but at a lower frequency. In the comparison between the buffer treated

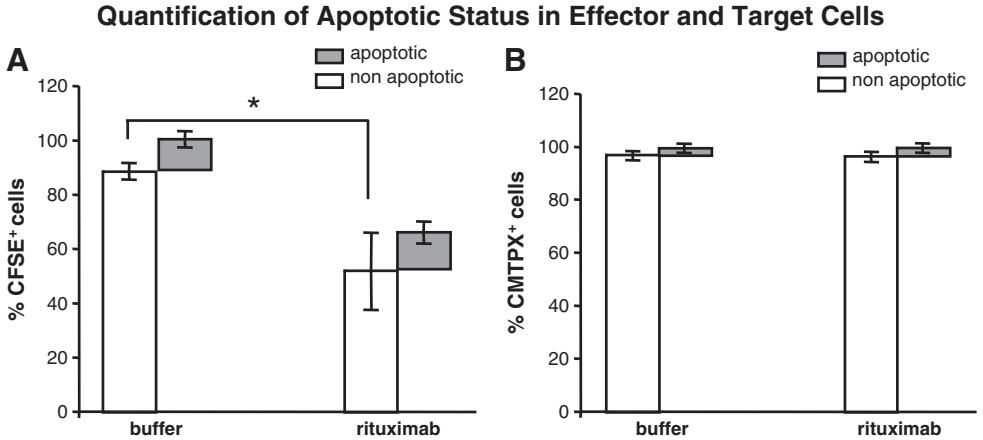

Fig. 4. Apoptotic status of target and effector cells in the presence of rituximab. Using the ImageStream imaging flow cytometer we compared the percentage of recovery of Ramos target cells and U-937 effector cells in absence and presence of 5 μg/ml rituximab after two hour incubation time. Panel A shows the percentage of apoptotic (gray) and non-apoptotic (white) CFSE$^+$ Ramos cells incubated with U-937 effector cells and in the presence or absence or rituximab. Panel B shows the percentage of apoptotic (gray) and non-apoptotic (white) U-937 cells CMTPX$^+$ incubated with Ramos cells and in the presence or absence or rituximab. Error bars indicate standard deviation of three independent experiments and (*) *t*-test $p \leq 0.05$.

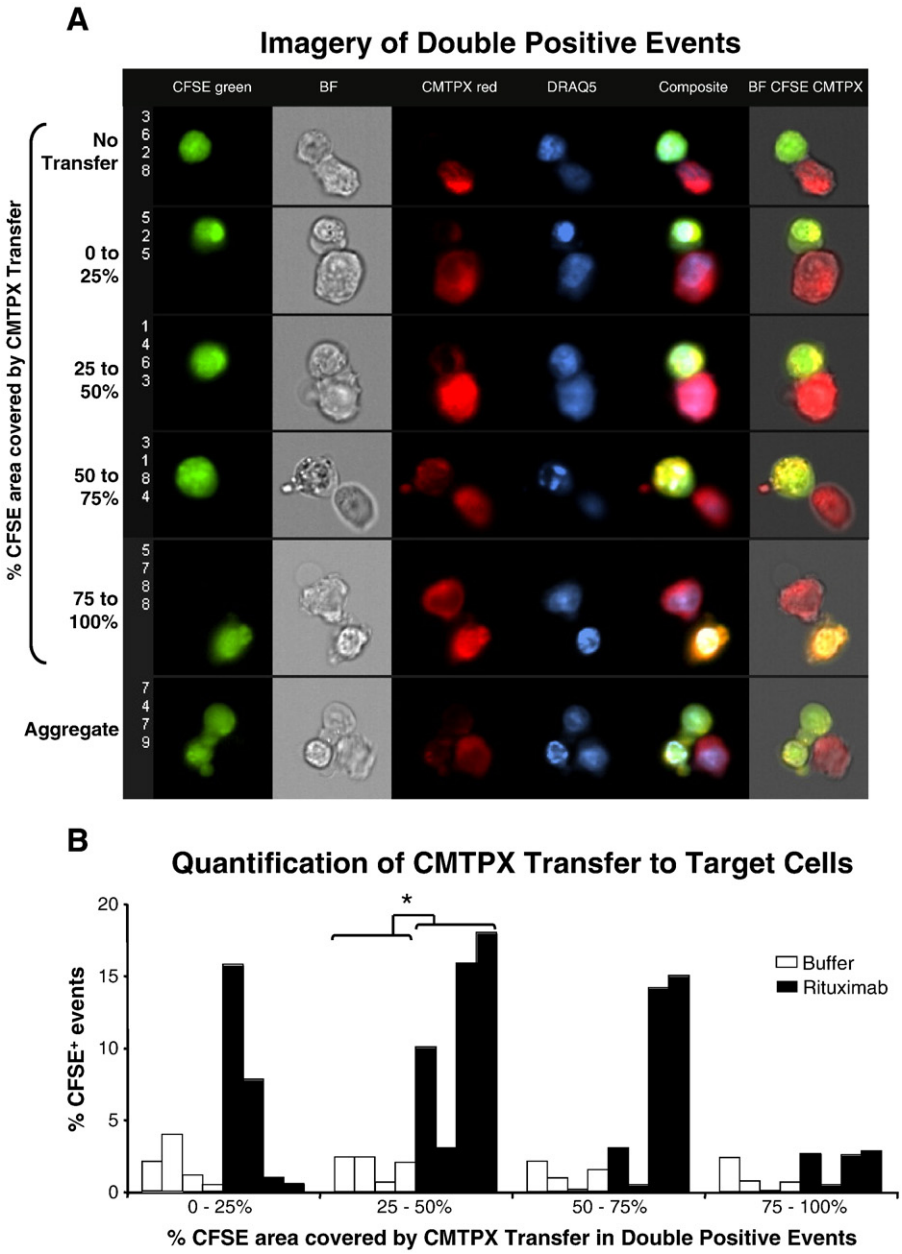

Fig. 5. Analysis of cytoplasmic transfer from effector cells to target cells in double positive events. We used an ImageStream multispectral system and acquired a total of 10,000 events to study the double positive events containing Ramos cells stained with CFSE and U-937 cells stained with CMTPX after incubation for 1 h in the absence and presence of rituximab. Panel A shows imagery of double positive events including CFSE fluorescence, brightfield, CMTPX fluorescence, DRAQ5 fluorescence, a composite image of fluorescent stain, and an overlay of brightfield, red and green fluorescence. In the descending rows we show representative imagery of double positive events with increasing percentage of green ($CFSE^+$) masked region covered by red ($CMTPX^+$) mask, evidence of cytoplasmic transfer from effector to target cells. At the bottom we show representative imagery of an aggregate of multiple target cells and an effector cell. Panel B shows the percentage of $CFSE^+$ events with different percentages of CFSE area covered by CMTPX fluorescence comparing buffer treatment (open bars) and rituximab (black bars). Each bar corresponds to different experiments and (*) *t*-test $p \leq 0.05$.

condition and rituximab treatment, there is a significant increase in the proportion of target cells with cytoplasmic signal covered 25–50% from effector cells in the presence of the antibody (Fig. 5B). The presence of aggregates is also expected, since the generation of homotypic aggregates of Ramos cells mediated by rituximab have been previously reported (Jazirehi et al., 2007).

3.5. Image analysis of interacting effector/target cells

In order to quantify the proportion of phagocytic events in the context of effector and target cells incubated in the presence of a therapeutic antibody or ADCP activity, we used the IDEAS® package to calculate the delta centroid XY. This parameter provides the absolute distance between the

centers of the mask generated for the red signal to the center of the mask of the green signal in a double positive event (Fig. 6A). Therefore, when the distance between the centers of the effector and target cells is less than half the radius of the masks they reach a "phagocytic threshold", in which the effector cell is engulfing the target cell. The histogram of delta centroid XY distribution of the double positive events allow the estimation of phagocytic events that would be expected between effector and target cells in ADCP activity (Fig. 6B). We can see that of 10,000 events acquired of U-937 cells and Ramos cells incubated for 2 h in the presence of 5 μg/ml rituximab, only 10 events are in the phagocytic range. The arrows pointing down show representative imagery of an event inside the phagocytic threshold and of events beyond the phagocytic threshold. In the case inside the phagocytic threshold, the green signal overlaps completely with the red, suggesting that this event may be a target cell in which cytoplasmic material from an effector cell has been transferred, in which case we cannot count the event as true phagocytosis. In fact, under the conditions studied we could not detect phagocytic events in which we could observe clearly a complete target cell inside of an effector cell. This observation can be explained by the fact that in most of the effector/target cell events there is some transfer of cytoplasmic material from the effector to the target cell and, since these interactions are transient, we can expect to observe some double positive events with total overlapping of fluorophores.

4. Discussion

This method provides a more complete picture of the events associated with ADCC activity than standard flow cytometry. It allows the simultaneous determination of the apoptotic index of effector and target cells, the quantification of healthy target cells, the visualization of the characteristics

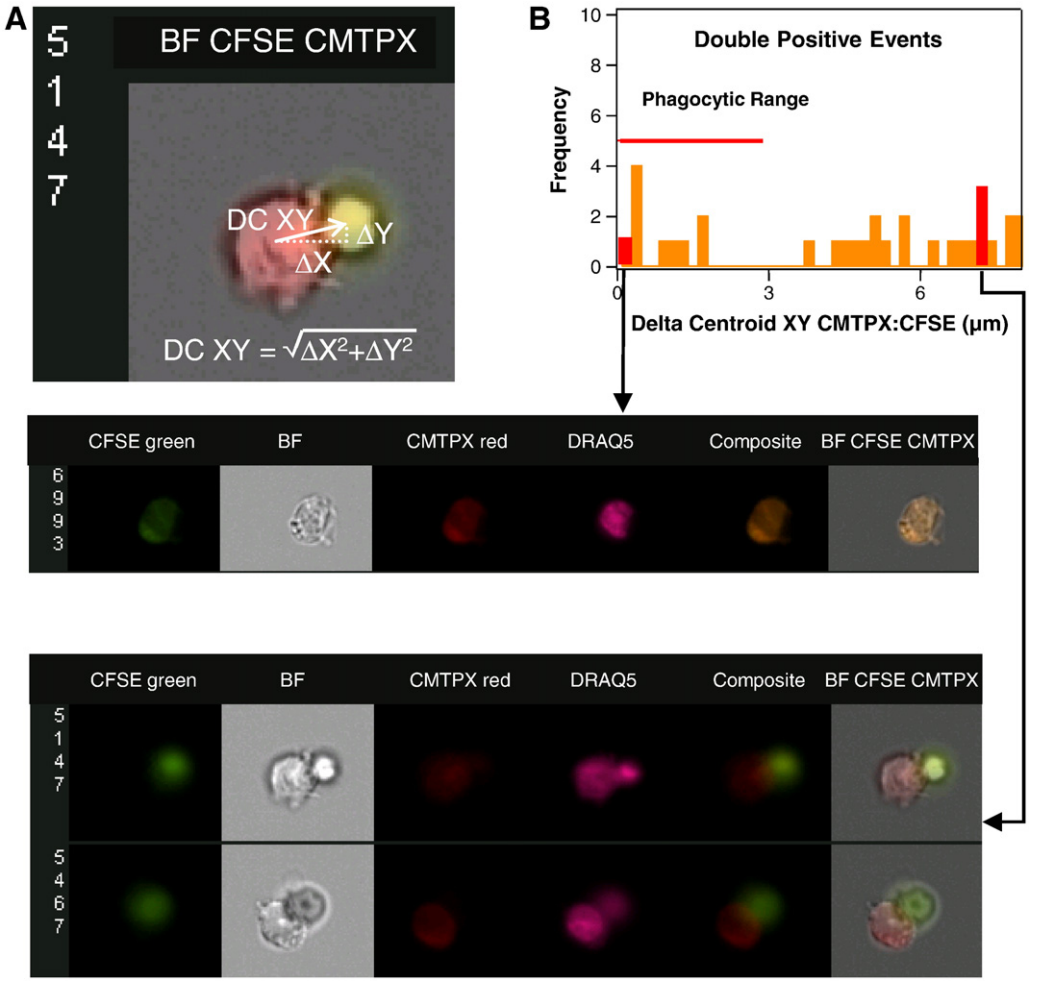

Fig. 6. Delta centroid image analysis to identify phagocytosis in double positive events. Panel A shows a composite image of brightfield, CFSE, and CMTPX fluorescence in a double positive event of U-937 effector cells and Ramos target cells incubated for 2 h in the presence of 5 μg/ml rituximab. Superimposed is the vector used to calculate the distance between the centers of the masks of the effector and the target cell. At the bottom of the image is the equation to calculate the delta centroid XY. Panel B shows a frequency histogram of the delta centroid XY distances of the double positive events. We set a threshold of 3 μm for the delta centroid XY as the phagocytic range, to identify phagocytic events. Below we show imagery of an event inside the phagocytic range in which there is overlapping of green and red signal. At the bottom we show imagery of events in which there is just contact of effector and target cells, resulting in the delta centroid distance equaling the sum of the radii of the green and red fluorescent events (values well beyond the phagocytic range).

of the interaction between effector and target cells, the formation of the cytotoxic synapse, cytoplasmic communication, and finally the quantitative analysis of rare events such as phagocytosis of the target cell.

Treatment with rituximab, the first monoclonal antibody approved by the Food and Drug Administration for the treatment of human cancer, is now routinely used for the treatment of non-Hodgkin's lymphoma. Unlike conventional approaches for the detection of ADCC events that rely on quantification of the release of traceable compounds from target cells or flow cytometry analysis of population-wide phenomena, the current work offers a novel and more comprehensive perspective of effector–target cell interactions during ADCC events. Studies in breast cancer suggest that under physiological conditions in which high E:T ratios are not frequent, apoptosis induction is expected to be the main pathway of cell death mediated by ADCC (Stockmeyer et al., 2003).

Apoptotic cell death is characterized by a series of events that include caspase activation, cell shrinkage, membrane blebbing, cleavage of nuclear DNA and chromatin condensation (Cohen, 1993). The morphologic characteristics are easily observed by optical microscopy, but their quantitative measurement can be time consuming and difficult to reproduce because of the lack of objectivity and throughput limitations. We observe a reduction in the number of gated target cells in the presence of rituximab compared to control, an evidence of their destruction by ADCC activity. We also evaluated the apoptotic index of the remaining cells. The detection of Annexin V bound to phosphatidylserine exposed on the surface of the apoptotic cells by flow cytometry is a standard quantitative relatively unbiased method to determine the apoptotic index. However, studies in NHL primary cells treated with rituximab have shown that this antibody generates aggregates that exhibit high Annexin V staining, which does not correlate with apoptosis and cannot be taken as a reliable marker of rituximab-induced apoptosis (Manches et al., 2003). Recent studies using automated imaging analysis with morphology-based algorithms applied to multispectral imagery acquired by imaging flow cytometry provide a reproducible, robust and comprehensive analysis of apoptosis of a large population of cells (Henery et al., 2008). This method correlates highly with standard flow cytometric measurement of apoptosis by Annexin V and caspase activation, with the advantage that imaging analysis does not rely on the binding of a compound to a cell surface marker, allowing more accurate exclusion of necrotic cells and the detection of earlier apoptosis events (Henery et al., 2008). Another advantage of the analysis using images of both effector and target cells is that it allows the generation of digital masks to segregate clearly both populations of cells even in double positive events for accurate quantification and analysis of their apoptotic index. In contrast, standard flow cytometric methods such as Annexin V binding cannot discriminate which cell is apoptotic in a dimeric complex: a) the effector, b) the target, or c) both effector and target cells, and assign a false positive apoptotic event to both effector and target cell population. We have demonstrated that imaging flow cytometry can be used for the determination of ADCC activity by quantification of total number of target and effector cells, as well as the apoptotic index of both cell populations.

Studies of ADCC activity have shown that this event is associated with an intimate interaction between the effector cell and the target cell, including mutual exchange of membrane lipids, the formation of the “cytotoxic synapse” (Stockmeyer et al., 1996; Horner et al., 2007), an interaction involved in triggering programmed cell death in the target cell (Horner et al., 2007), and with the process of trogocytosis, in which the targeted epitopes are shaved from the surface of the tumor cell and transferred with membrane fragments to the effector cells (Megjugorac et al., 2007; Beum et al., 2008). The transient aggregate formation could be detected also in the absence of antibody, but this interaction was extended in the presence of an antibody targeting the Fc receptor and the tumor-associated antigen (Horner et al., 2007). In our case, this heterotypic aggregation can be clearly visualized in the double positive events between effector U-937 and Ramos cells. Although we did not directly stain the membranes of the effector and target cells, the imaging analysis allows us to observe transfer of cytoplasmic content from fluorescently labeled effector cells to the target cells in double positive events, either in the presence or absence of rituximab, with the proportion of transfer much larger in the presence of rituximab. Other studies have shown the generation of a cytoplasmic communication between effector and target cells (Horner et al., 2007). Although we do not know the nature of the cytoplasmic material transferred, we can speculate that it may contain lytic factors that may contribute to target cell death.

Although ADCC activity has been reported to be a major player in the anti-tumor activity of therapeutic antibodies, studies using M-CSF differentiated human macrophages have shown that rituximab can mediate ADCP against human B-chronic lymphocytic leukemia target cells in vitro (Leidi et al., 2009). Other studies have shown that rituximab can mediate ADCC, ADCP and apoptosis of non-Hodgkin's lymphoma primary cells in vitro (Manches et al., 2003). We used the delta centroid XY analysis to estimate the frequency of phagocytic events. Although the population of double positive events was significant either with rituximab or buffer, the occurrence of phagocytosis under these conditions was very rare, and in consequence we could not quantify ADCP activity properly. However, this study demonstrates the feasibility of the application of the ImageStream technology to evaluate simultaneously the ADCC and ADCP activities of therapeutic antibodies against cancer cells in vitro. It is possible that with other effector cells and/or target cells ADCP events will be more frequently observed. It is expected that similar studies with different cell populations, such as peripheral blood mononuclear cells, would allow the identification of different effector cell populations interacting preferentially with the targeted cancer cells. Another potential application of this technology would be in a clinical setting, to identify those patients who would be expected to be poor responders, based on poor ADCC responses mediated by a therapeutic monoclonal antibody. This individualized assessment would allow clinicians to tailor treatment based on the patient's ADCC responses. It has been reported that the clinical efficacy of cetuximab is correlated with polymorphisms in Fcγ receptors expressed on the patient's lymphocytes (Taylor et al., 2009), although this correlation is not absolute for all antibodies and is not observed in all malignancies (Ferris et al., 2010). This suggests that direct measurement of ADCC may provide better prognostic

information than assessment of Fcγ polymorphisms. However, testing this activity in primary cells from patients may be more difficult than testing this activity against a standard cell line such as Ramos, since the dissociation and staining of the primary cancer cells may affect their surface integrity and viability, compromising the interpretation of the results. Certainly, further studies will be needed to confirm the clinical utility of this technology.

In conclusion, we show that this method allows a detailed observation of the physical interaction between target and effector cells, their morphological changes, level of apoptosis, and the determination of an exchange of their cytosolic contents. Unlike conventional approaches for the detection of ADCC events, the current work combines the statistical power of flow cytometry with the analytical advantages of cell imaging, providing a novel tool to better evaluate the effector/target cell interactions during ADCC. Since this activity is relevant also in the protection against viral infections, parasitic and bacterial diseases (Hashimoto et al., 1983; Moore et al., 2002), the direct visualization of the biological activity of antibodies in the context of effector/target cell interactions using imaging in flow cytometry, is of interest for the characterization and pre-clinical evaluation of antibody therapeutics at large, as well as for better defining mechanisms involved in effector responses to host antibodies against target cells.

Acknowledgments

The authors thank Dr. Tracy R. Daniels, University of California at Los Angeles, for critically reading the manuscript, and Raymond Kong and Ben Alderete for their technical assistance. These studies were supported by the NIH/NCI grants R01 CA107023, NIH/NCI R01 supplement CA107023-02S1 and CA57152-13S1, the Howard Hughes Medical Institute (HHMI) Gilliam Fellowship for Ph.D. studies, and the Whitcome Fellowship of the Molecular Biology Interdepartmental Ph.D. Program (MBIDP) at UCLA. GH is a member of the National Council for Scientific and Technological Research (CONICET), Argentina.

References

Beum, P.V., Lindorfer, M.A., Hall, B.E., George, T.C., Frost, K., Morrissey, P.J., Taylor, R.P., 2006. Quantitative analysis of protein co-localization on B cells opsonized with rituximab and complement using the ImageStream multispectral imaging flow cytometer. J. Immunol. Methods 317, 90.

Beum, P.V., Mack, D.A., Pawluzkowczkowycz, A.W., Lindorfer, M.A., Taylor, R.P., 2008. Binding of rituximab, trastuzumab, cetuximab, or mAb T101 to cancer cells promotes trogocytosis mediated by thp-1 cells and monocytes. J. Immunol. 181, 8120.

Brunner, K.T., Mauel, J., Cerottini, J.C., Chapuis, B., 1968. Quantitative assay of the lytic action of immune lymphoid cells on 51-Cr-labelled allogeneic target cells in vitro; inhibition by isoantibody and by drugs. Immunology 14, 181.

Cohen, J.J., 1993. Apoptosis. Immunol. Today 14, 126.

Dalle, S., Thieblemont, C., Thomas, L., Dumontet, C., 2008. Monoclonal antibodies in clinical oncology. Anticancer Agents Med. Chem. 8, 523.

Ferris, R.L., Jaffee, E.M., Ferrone, S., 2010. Tumor antigen-targeted, monoclonal antibody-based immunotherapy: clinical response, cellular immunity, and immunoescape. J. Clin. Oncol. 28, 4390.

George, T.C., Basiji, D.A., Hall, B.E., Lynch, D.H., Ortyn, W.E., Perry, D.J., Seo, M.J., Zimmerman, C.A., Morrissey, P.J., 2004. Distinguishing modes of cell death using the ImageStream multispectral imaging flow cytometer. Cytometry A 59, 237.

Glennie, M.J., French, R.R., Cragg, M.S., Taylor, R.P., 2007. Mechanisms of killing by anti-CD20 monoclonal antibodies. Mol. Immunol. 44, 3823.

Hashimoto, G., Wright, P.F., Karzon, D.T., 1983. Antibody-dependent cell-mediated cytotoxicity against influenza virus-infected cells. J. Infect. Dis. 148, 785.

Henery, S., George, T., Hall, B., Basiji, D., Ortyn, W., Morrissey, P., 2008. Quantitative image based apoptotic index measurement using multispectral imaging flow cytometry: a comparison with standard photometric methods. Apoptosis 13, 1054.

Horner, H., Frank, C., Dechant, C., Repp, R., Glennie, M., Herrmann, M., Bernhard Stockmeyer, B., 2007. Intimate cell conjugate formation and exchange of membrane lipids precede apoptosis induction in target cells during antibody-dependent, granulocyte-mediated cytotoxicity. J. Immunol. 179, 337.

Jakubek, P., Thorsby, E., Hirschberg, H., 1983. Cell mediated lympholysis; a modified technique using ^{111}indium-oxine-labelled targets. J. Immunol. Methods 60, 379.

Jazirehi, A.R., Vega, M.I., Bonavida, B., 2007. Development of rituximab-resistant lymphoma clones with altered cell signaling and cross-resistance to chemotherapy. Cancer Res. 67, 1270.

Karagiannis, S.N., Bracher, M.G., Hunt, J., McCloskey, N., Beavil, R.L., Beavil, A.J., Fear, D.J., Thompson, R.G., East, N., Burke, F., Moore, R.J., Dombrowicz, D.D., Balkwill, F.R., Gould, H.J., 2007. IgE-antibody-dependent immunotherapy of solid tumors: cytotoxic and phagocytic mechanisms of eradication of ovarian cancer cells. J. Immunol. 179, 2832.

Kim, G.G., Donnenberg, V.S., Donnenberg, A.D., Gooding, W., Whiteside, T.L., 2007. A novel multiparametric flow cytometry-based cytotoxicity assay simultaneously immunophenotypes effector cells: comparisons to a 4 h 51Cr-release assay. J. Immunol. Methods 325, 51.

Leidi, M., Gotti, E., Bologna, L., Miranda, E., Rimoldi, M., Sica, A., Roncalli, M., Palumbo, G.A., Introna, M., Golay, J., 2009. M2 macrophages phagocytose rituximab-opsonized leukemic targets more efficiently than m1 cells in vitro. J. Immunol. 182, 4415.

Manches, O., Lui, G., Chaperot, L., Gressin, R., Molens, J.P., Jacob, M.C., Sotto, J.J., Leroux, D., Bensa, J.C., Plumas, J., 2003. In vitro mechanisms of action of rituximab on primary non-Hodgkin lymphomas. Blood 101, 949.

Megjugorac, N.J., Jacobs, E.S., Izaguirre, A.G., George, T.C., Gupta, G., Fitzgerald-Bocarsly, P., 2007. Image-based study of interferongenic interactions between plasmacytoid dendritic cells and HSV-infected monocyte-derived dendritic cells. Immunol. Invest. 36, 739.

Metelitsa, L.S., Gillies, S.D., Super, M., Shimada, H., Reynolds, C.P., Seeger, R.C., 2002. Antidisialoganglioside/granulocyte macrophage-colony-stimulating factor fusion protein facilitates neutrophil antibody-dependent cellular cytotoxicity and depends on FcgammaRII (CD32) and Mac-1 (CD11b/CD18) for enhanced effector cell adhesion and azurophil granule exocytosis. Blood 99 (11), 4166.

Moore, T., Ananaba, G.A., Bolier, J., Bowers, S., Belay, T., Eko, F.O., Igietseme, J.U., 2002. Fc receptor regulation of protective immunity against *Chlamydia trachomatis*. Immunology 105, 213.

Stockmeyer, B.V.T., Repp, R., Deo, Y., van de Winkel, J.G.J., Kalden, J.R., Gramatzki, M., 1996. Cell adhesion molecules cooperate with Fc-{gamma}-RI in ADCC of G-CSF primed neutrophils against breast cancer cells. Blood 88.

Stockmeyer, B., Beyer, T., Neuhuber, W., Repp, R., Kalden, J.R., Valerius, T., Herrmann, M., 2003. Polymorphonuclear granulocytes induce antibody-dependent apoptosis in human breast cancer cells. J. Immunol. 171, 5124.

Taylor, R.J., Chan, S.L., Wood, A., Voskens, C.J., Wolf, J.S., Lin, W., Chapoval, A., Schulze, D.H., Tian, G., Strome, S.E., 2009. FcgammaRIIIa polymorphisms and cetuximab induced cytotoxicity in squamous cell carcinoma of the head and neck. Cancer Immunol. Immunother. 58, 997.

Wang, S.Y., Weiner, G., 2008. Complement and cellular cytotoxicity in antibody therapy of cancer. Expert Opin. Biol. Ther. 8, 759.

Wisecarver, J., Bechtold, T., Collins, M., Davis, J., Lipscomb, H., Sonnabend, J., Purtilo, D.T., 1985. A method for determination of antibody-dependent cellular cytotoxicity (ADCC) of human peripheral mononuclear cells. J. Immunol. Methods 79, 277.